

 Open access • Journal Article • DOI:10.1103/PHYSREVA.39.4628

Destruction of quantum coherence in a nonlinear oscillator via attenuation and amplification. — Source link

D. J. Daniel, Gerard J. Milburn

Institutions: Australian National University, University of Queensland

Published on: 01 May 1989 - Physical Review A (American Physical Society)

Topics: Master equation, Coherence (physics), Squeezed coherent state, Quantum optics and Attenuation

Related papers:

- [Dissipative quantum and classical Liouville mechanics of the anharmonic oscillator.](#)
- [Generating quantum mechanical superpositions of macroscopically distinguishable states via amplitude dispersion.](#)
- [Quantum and classical Liouville dynamics of the anharmonic oscillator.](#)
- [Exact quantum statistics of a nonlinear dissipative oscillator evolving from an arbitrary state.](#)
- [Third-order nonlinear dissipative oscillator with an initial squeezed state](#)

Share this paper:    

View more about this paper here: <https://typeset.io/papers/destruction-of-quantum-coherence-in-a-nonlinear-oscillator-4pl6jq02mp>

Destruction of quantum coherence in a nonlinear oscillator via attenuation and amplification

D. J. Daniel

*Department of Theoretical Physics, Research School of Physical Sciences, Australian National University,
Australian Capital Territory, Canberra, 2601, Australia*

G. J. Milburn

Department of Physics, University of Queensland, Saint Lucia, Queensland 4067

(Received 17 November 1988)

The exact solution to the master equation of a nonlinear oscillator, subject to damping or amplification, is presented. The effect of such incoherent processes on the quantum-coherence properties and recurrences is obtained. It is shown that amplification destroys quantum coherence more rapidly than does attenuation.

INTRODUCTION

In a number of recent papers^{1,2} a simple exactly solvable nonlinear oscillator model has been studied that shows how quantum coherences lead to a recurrence of the initial quantum state and a departure of the quantum dynamics from that expected classically. Indeed it was shown by Yurke and Stoler³ that this model may be used to generate a quantum superposition of two oscillator coherent states with macroscopically distinguishable amplitudes. However, as many authors have noted,⁴⁻⁸ such quantum superposition states and quantum-coherence features, in general, are extremely sensitive to external fluctuations. Milburn and Holmes² considered the effects of dissipation on the recurrences of this nonlinear oscillator model and showed that even very weak damping is sufficient to destroy quantum-coherence effects and restore classical behavior as the action of the initial state approaches the semiclassical limit. A similar result was found by Yurke and Stoler using different techniques.³ In Ref. 2 dissipation was included by coupling the oscillator to a zero-temperature heat bath. In this paper we extend that work to treat the case of a heat bath at a nonzero temperature. A slight modification of the model also allows us to determine the effect of amplification on quantum coherence.

The nonlinear oscillator model discussed here exhibits a number of the characteristic features of nonlinear quantum systems, such as recurrences, squeezing, and interference effects in the marginal distributions of the position and momentum. It also provides a simple illustration of interference in phase space, a concept recently employed by Schleich and Wheeler⁹ to explain the oscillations in the tail of the photon number distribution for squeezed light. We will determine the effect of attenuation and amplification on each of these effects. Our results indicate that such characteristic quantum features are extremely sensitive to any attenuation or amplification. In particular, quantum recurrences are suppressed at a rate which becomes very large as the initial average energy of the system approaches the semiclassical limit (that is,

large compared to $\hbar\omega_0$ where ω_0 is the fundamental frequency of the linear part of the oscillator).

Our method is based on a master equation which is expected to be valid for small nonlinearities and weak coupling to the external degrees of freedom of the attenuator or amplifier. The master equation, an equation of motion for the system density operator, is then converted to an equivalent *c*-number evolution equation for the diagonal elements of the density operator in the coherent-state basis. Such a matrix element is in fact a true joint probability density for a special class of simultaneous measurement of position and momentum, and is known as the *Q* function¹⁰ and in other contexts as the Husimi function.¹¹ The resulting evolution equation is a nonlinear second-order partial differential equation. It is similar in some respects to a Fokker-Planck equation¹² but cannot strictly be interpreted as such as the diffusion matrix is not positive definite (in fact, it is complex). We solve this equation exactly using techniques which may be of interest for the solution of other nonlinear second-order partial differential equations of this type. Once the *Q* function is obtained all moments and marginal distributions may be calculated. The *Q* function itself illustrates a number of important features of the model.

I. NONLINEAR OSCILLATOR MODEL

We take as our nonlinear oscillator model a system described by the Hamiltonian¹

$$H = H_0 + \frac{\mu}{\hbar\omega_0} H_0^2, \quad (1.1)$$

where

$$H_0 = \frac{1}{2}(p^2 + \omega_0^2 q^2)$$

is the free Hamiltonian for a simple harmonic oscillator. This model could describe a cavity-field mode interacting with a Kerr nonlinear medium.¹³ A comparison of the quantum and classical dynamics of this model is given in Ref. 1, and we summarize some of those results here. A

convenient way to compare the quantum and classical dynamics is through the joint phase-space probability density describing simultaneous measurement of position and momentum. In classical mechanics the definition of such a distribution is straightforward; it is simply a joint probability density on phase space. However, in quantum mechanics one must proceed more carefully as the operators for position and momentum do not commute. Nonetheless such measurements can be described^{10,14} and lead to a class of joint probability densities which form a subclass of classical joint distributions. The quantum distributions cannot have too small an area of support on phase space, a reflection of the uncertainty principle. For a particular model of such measurements the resulting distribution is the Q function defined by

$$Q(\alpha) = \langle \alpha | \hat{\rho} | \alpha \rangle, \quad (1.2)$$

where $|\alpha\rangle$ is a Glauber coherent state and the complex variable α is related to the position and momentum variables by

$$\alpha = \left[\frac{\omega_0}{2\hbar} \right]^{1/2} q + i(2\hbar\omega_0)^{-1/2} p. \quad (1.3)$$

One easily verifies the $Q(\alpha)$ is bounded by unity, is positive, and is normalized with respect to the measure $d^2\alpha/\pi$.

If the initial classical state is chosen to be the density

$$Q(\alpha, 0) = \exp(-|\alpha - \alpha_0|^2), \quad (1.4)$$

a Gaussian centered at α_0 , the average value of α decays to zero under Liouville evolution of the density. The initial circular contours of the Gaussian undergo a rotational shear about the origin. However, if we choose an initial quantum state with the corresponding Q function given by Eq. (1.4) (that is, we choose the initial state to be the coherent state $|\alpha_0\rangle$), something quite different occurs. The dynamics in this case is governed by the Schrödinger equation. For short times the dynamics of the Q function mimics the classical result, undergoing a rotational shear. This feature of the dynamics has been discussed by Kitagawa *et al.* in the context of quantum optics.¹³ However, as the leading edge of the sheared distribution begins to encircle the trailing tail phase-space interference features arise. These interference features are due to the underlying quantum coherence between the energy eigenstates of H_0 superposed to form the initial state.¹⁵ This interference effect is shown in an early stage in Fig. 1, in which the Q function is plotted as a function of the real and imaginary parts of α . The origin is in the center of the figure and the leading edge of the sheared density is toward the foreground. The peaks and hollows in the foreground are interference fringes between the leading edge and the trailing tail of the density. At the time $t = \pi/2\mu$ (in a frame rotating at frequency ω_0) the system evolves to the coherent superposition state

$$|\psi\rangle = \frac{1}{\sqrt{2}}(e^{-i\pi/4}|\alpha_0\rangle + e^{i\pi/4}|-\alpha_0\rangle). \quad (1.5)$$

This surprising result has been discussed by Yurke and

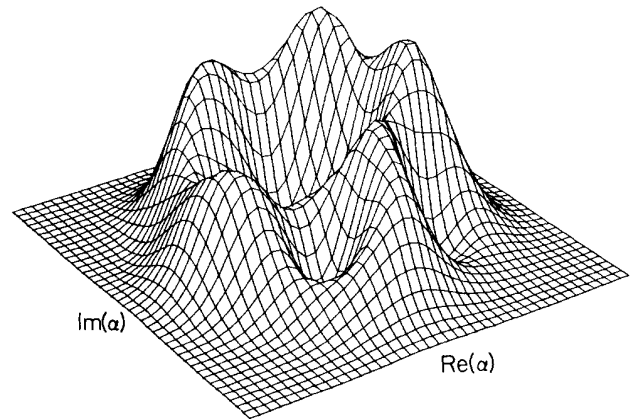


FIG. 1. Plot of the Q function for the nonlinear oscillator with no dissipation, against the real and imaginary parts of α . The leading edge of the sheared density is in the foreground and is moving in a clockwise direction. The origin is at the center, $\alpha_0 = 2.0$, $\nu = 1.8$, $\bar{\kappa} = 0$.

Stoler.³ At times such that $t = \pi/\mu$ the system evolves to the state $|\alpha_0\rangle$, that is, the initial state has recurred up to a phase of π . The entire process then repeats until the initial state has been reconstructed at $t = 2\pi/\mu$. The model thus provides a very clear illustration of how quantum dynamics departs from short-time mimicry of classical behavior.

The behavior of the quantum density is reflected in the momenta. In Fig. 2 we have plotted the average value of the amplitude on phase-space over the time interval $0 \leq t \leq 2\pi/\mu$. Also shown for comparison is the corresponding classical result (dashed line). The close similarity

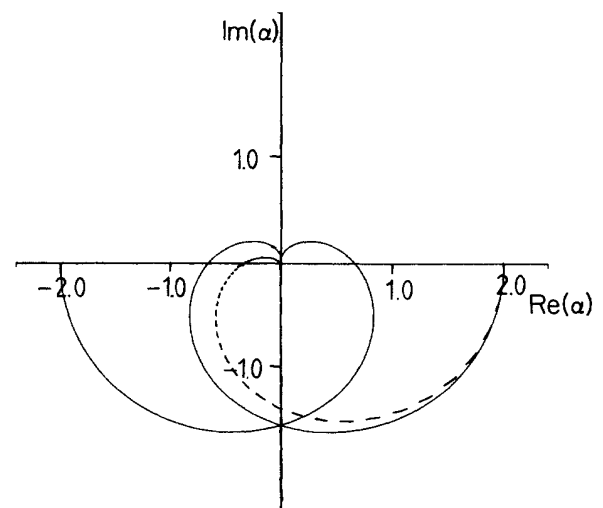


FIG. 2. Plot of the average trajectory in phase space, that is, the real part of $\langle a(\tau) \rangle$ vs the imaginary part, over the time interval $0 \leq \nu \leq 2\pi$. The dashed line represents the corresponding classical case. $\alpha_0 = 2.0$, $\bar{\kappa} = 0$.

ty of quantum and classical behavior for short times is clearly evident, as is the recurrence of the initial quantum state at $-\alpha_0$. One may also calculate the variances in quantity x_1 and x_2 defined by

$$x_1 = (\alpha + \alpha^*)/2, \quad (1.6)$$

$$x_2 = (\alpha - \alpha^*)/2. \quad (1.7)$$

In the classical description the variances saturate as the initial density becomes wrapped around the origin. In Fig. 3 we plot the classical and quantum variances in x_1 . The initial correspondence of the classical and quantum result is once again evident. Note that the quantum result, however, drops below the classical result at $t = \pi/2\mu$, the time at which the superposition state in Eq. (1.5) forms. In fact, at this time the variance falls below the initial coherent-state value, a result known as squeezing.¹⁶ It should be noted that the variances of x_1 and x_2 computed directly from the Q function are not identical to the variances in the corresponding dimensionless position and momentum operators \hat{X}_1 and \hat{X}_2 defined by

$$\hat{X}_1 = \left[\frac{\omega_0}{2\hbar} \right]^{1/2} \hat{q}, \quad (1.8)$$

$$\hat{X}_2 = (2\hbar\omega_0)^{-1/2} \hat{p}. \quad (1.9)$$

This is because the Q function gives directly the moments of "approximate" position and momentum variables. This is the price paid for a simultaneous measurement of noncommuting observables. In fact, the variances in x_i and \hat{X}_i are related by

$$V(x_i) = V(\hat{X}_i) + \frac{1}{4}. \quad (1.10)$$

In quantum optics one would say that the Q function gives directly the antinormally ordered moments¹⁷ of the creation and destruction operators. This result leads to Eq. (1.10) in the case of the variance in \hat{X}_i .

Another way to see the effect of interference in phase space is to explicitly calculate the marginal distributions for the dimensionless position and momentum operators \hat{X}_1 and \hat{X}_2 . These are given in terms of the Q -function amplitudes, $\langle \alpha | \psi \rangle$, for the state $|\psi\rangle$ as

$$P(X_i) = \left| \int d^2\alpha \frac{1}{\pi} \langle X_i | \alpha \rangle \langle \alpha | \psi \rangle \right|^2, \quad (1.11)$$

where the state $|X_i\rangle\langle X_i|$ is the resolution of identity for \hat{X}_i . Equation (1.11) can be viewed as the quantum generalization of the classical result

$$P(X_i) = \int d^2\alpha \frac{1}{\pi} \delta^{(2)}(X_i - x_i) Q(\alpha), \quad (1.12)$$

where x_i are defined in Eqs. (1.6) and (1.7), and $Q(\alpha)$ is a classical joint phase-space probability density describing the system state. In Eq. (1.11), $\langle \alpha | \psi \rangle$ is the amplitude for a simultaneous measurement of position and momentum to give a particular result α , while $\langle X_i | \alpha \rangle$ is the conditional amplitude that this result corresponds to a position or momentum X_i . Thus the quantum result is constructed in the same way as the classical result but at the

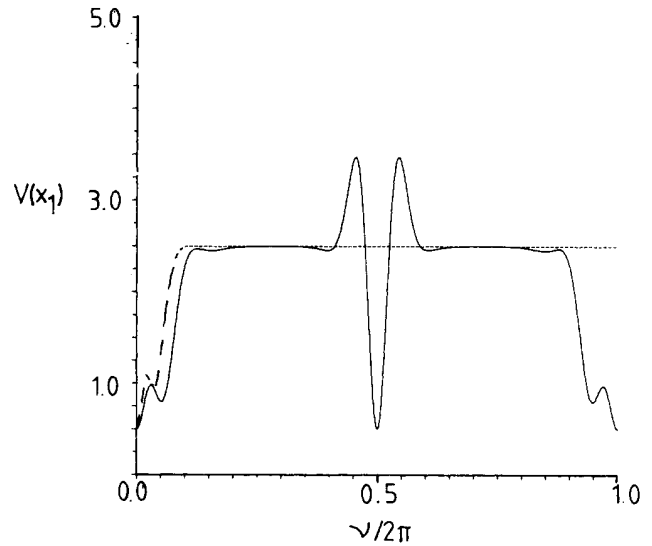


FIG. 3. Plot of the classical (dashed line) and quantum (solid line) variance in x_1 , against $v/2\pi$, with no dissipation. $\alpha_0 = 2.0$, $\bar{\kappa} = 0$.

level of probability amplitudes rather than probabilities, a feature of quantum mechanics emphasized by Feynman.¹⁸

For the special case of the superposition state given in Eq. (1.5) the marginal distribution for X_1 is

$$P(X_1) = \frac{1}{2} [P_+(X_1) + P_-(X_1)] + 2\sqrt{P_+(X_1)P_-(X_1)\sin(4X_1r_0\sin\theta_0)}, \quad (1.13)$$

where

$$P_{\pm}(X_1) = \left[\frac{2}{\pi} \right]^{1/2} \exp[-2X_1^2 - |\alpha_0|^2 \mp 2X_1(\alpha_0 - \alpha_0^*) - \frac{1}{2}(\alpha_0^2 + \alpha_0^{*2})]$$

and we have set $\alpha_0 = r_0 e^{i\theta_0}$. The distribution for \hat{X}_2 is given by

$$P(X_2) = \frac{1}{2} [P_+(X_2) + P_-(X_2)] + 2\sqrt{P_+(X_2)P_-(X_2)\sin(4X_2r_0\sin\theta_0)}, \quad (1.14)$$

where

$$P_{\pm}(X_2) = \left[\frac{2}{\pi} \right]^{1/2} \exp[-2X_2^2 - |\alpha_0|^2 \mp 2iX_2(\alpha_0 - \alpha_0^*) - \frac{1}{2}(\alpha_0^2 + \alpha_0^{*2})].$$

For imaginary α_0 $P(X_2)$ consists of a superposition of two Gaussian peaks centered at $\pm|\alpha_0|$; however, $P(X_1)$ consists of a single Gaussian at $X_1 = 0$ modulated by the interference term $1 + \sin(4X_2r_0)$.

In Figs. 4(a) and 4(b) we plot the marginal distributions for X_1 and X_2 at $t = \pi/2\mu$ for $\alpha_0 = i$. [At this time the superposition state in Eq. (1.5) has formed.] We clearly see interference features in the distribution for X_1 but not X_2 . These results may be interpreted in terms of the "interference in phase space" concept developed by Schleich and Wheeler.^{9,10}

The nonlinear oscillator model described by the Hamiltonian in Eq. (1.1) illustrates well the significant differences between the quantum and classical descriptions. In Sec. II we consider the effect of attenuation and amplification on the quantum features discussed above.

II. ATTENUATION AND AMPLIFICATION

We will model the effect of attenuation and amplification by coupling the nonlinear oscillator to a reservoir of oscillators assumed to be in thermal equilibrium at some temperature. We shall refer to this collection of oscillators as the bath. This is a standard approach to linear attenuation and amplification.^{17,19} The coupling between the nonlinear oscillator and the bath is described by the Hamiltonian

$$H_I = \hbar[a\Gamma^\dagger(t) + a^\dagger\Gamma(t)], \quad (2.1)$$

where a is the lowering operator for the nonlinear oscillator. The bath operators $\Gamma(t)$ are given by

$$\Gamma(t) = \sum_j g_j b_j e^{-i\omega_j t} \quad (2.2)$$

in the case of attenuation, and

$$\Gamma(t) = \sum_j g_j b_j^\dagger e^{i\omega_j t} \quad (2.3)$$

in the case of amplification. The sum is over all the bath oscillators and g_j is a coupling constant. The form of $\Gamma(t)$ for amplification makes it clear that we are considering a form of parametric amplification in which g_j plays the role of a pump field amplitude, while a and b_j play the role of signal and idler fields, respectively.

Standard methods¹⁷ lead to a master equation for the system density operator in the interaction picture:

$$\begin{aligned} \frac{d\hat{\rho}}{dt} = & -i\mu\omega_0((a^\dagger a)^2, \hat{\rho}) \\ & + \frac{\gamma}{2} [(2a\hat{\rho}a^\dagger - a^\dagger a\rho - \hat{\rho}a^\dagger a) \\ & + \gamma\bar{n}(a^\dagger\hat{\rho}a + a\hat{\rho}a^\dagger - a^\dagger a\rho - \hat{\rho}aa^\dagger)] \end{aligned} \quad (2.4)$$

in the case of attenuation and

$$\begin{aligned} \frac{d\hat{\rho}}{dt} = & -i\mu\omega_0((a^\dagger a)^2, \hat{\rho}) \\ & + \frac{\gamma}{2} [(2a^\dagger\hat{\rho}a - aa^\dagger\hat{\rho} - \rho aa^\dagger) \\ & + \gamma\bar{n}(a\hat{\rho}a^\dagger + a^\dagger\hat{\rho}a - aa^\dagger\rho - \hat{\rho}aa^\dagger)] \end{aligned} \quad (2.5)$$

for the case of amplification. In Eqs. (2.4) and (2.5) \bar{n} is the average number of bath quanta, and $\gamma/2$ is the attenuation or amplification constant. It should be noted that for $\bar{n} \neq 0$ the validity of Eqs. (2.4) and (2.5) depends on the nonlinearity μ being quite small.²⁰

To make a little clearer the role of γ we evaluate the mean of a for the case $\bar{n} = 0$ and $\mu = 0$. In the case of the attenuator one has

$$\langle a(t) \rangle = \langle a(0) \rangle e^{-\gamma t/2} \quad (2.6)$$

and for the amplifier

$$\langle a(t) \rangle = \langle a(0) \rangle e^{\gamma t/2}. \quad (2.7)$$

In the latter case we may thus view $e^{\gamma t}$ as the linear energy gain.

Equations (2.4) and (2.5) may be converted to equivalent c -number equations for the Q function. The appropriate techniques are described in Ref. 21. The results are

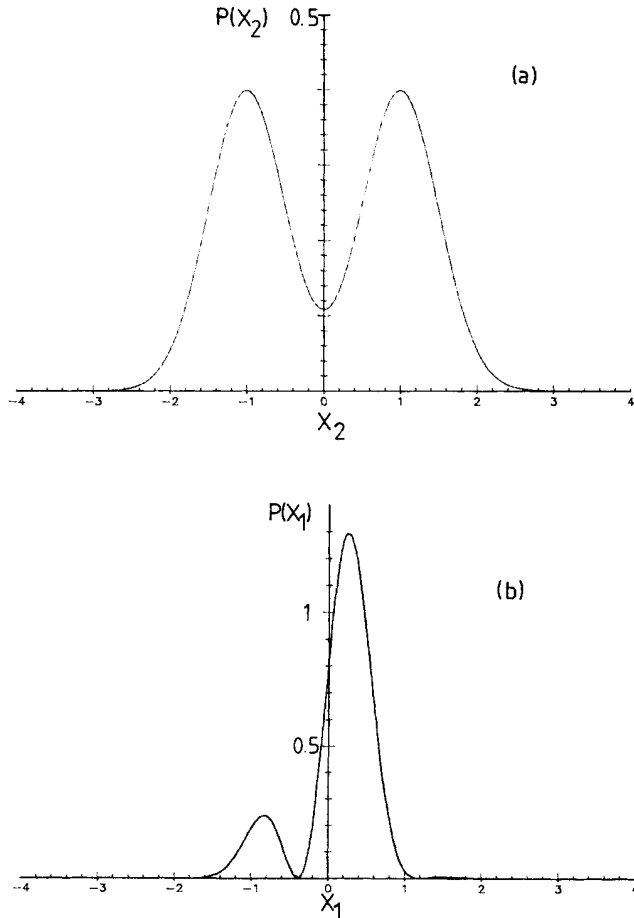


FIG. 4. Plot of the marginal distributions for \hat{X}_1 and \hat{X}_2 . (a) $P(X_2)$ vs X_2 ; (b) $P(X_1)$ vs X_1 . $\alpha_0 = i$, $\chi = 0$.

$$\begin{aligned} \frac{\partial Q}{\partial \tau} = & -i\mu \left[\alpha(1+2|\alpha|^2) \frac{\partial Q}{\partial \alpha} - \alpha^*(1+2|\alpha|^2) \frac{\partial Q}{\partial \alpha^*} + \alpha^2 \frac{\partial^2 Q}{\partial \alpha^2} - (\alpha^*)^2 \frac{\partial^2 Q}{\partial \alpha^{*2}} \right] + \frac{\kappa}{2} \left[\frac{\partial}{\partial \alpha} \alpha + \frac{\partial}{\partial \alpha^*} \alpha^* \right] Q \\ & + \kappa(\bar{n} + 1) \frac{\partial^2 Q}{\partial \alpha \partial \alpha^*} \end{aligned} \quad (2.8)$$

in the case of the attenuator, while

$$\frac{\partial Q}{\partial \tau} = -i\mu \left[\alpha(1+2|\alpha|^2) \frac{\partial Q}{\partial \alpha} - \alpha^*(1+2|\alpha|^2) \frac{\partial Q}{\partial \alpha^*} + \alpha^2 \frac{\partial^2 Q}{\partial \alpha^2} - (\alpha^*)^2 \frac{\partial^2 Q}{\partial \alpha^{*2}} \right] - \frac{\kappa}{2} \left[\frac{\partial}{\partial \alpha} \alpha + \frac{\partial}{\partial \alpha^*} \alpha^* \right] Q + \kappa\bar{n} \frac{\partial^2 Q}{\partial \alpha \partial \alpha^*} \quad (2.9)$$

in the case of amplification and we have defined the dimensionless variables $\tau = \omega_0 t$ and $\kappa = \gamma / \omega_0$. We now solve both of these equations for the initial condition

$$Q(\alpha, 0) = \exp(-|\alpha - \alpha_0|^2). \quad (2.10)$$

A. Attenuator

The solution to Eq. (2.8) subject to the initial condition (2.10) is (see the Appendix)

$$Q(\alpha, \tau) = \sum_{q,p=0}^{\infty} \frac{(\alpha\alpha_0^*)^q (\alpha^*\alpha_0)^p}{q! p!} e^{-Y_{p,q}(\tau)|\alpha|^2} R_{p,q}(\tau), \quad (2.11)$$

where

$$R_{p,q}(\tau) = \left[\frac{2\Delta e^{-v\Delta\bar{\kappa}/2}}{(\Omega + \Delta) - (\Omega - \Delta)e^{-v\Delta\bar{\kappa}/2}} \right]^{q+p+1} e^{v\bar{\kappa}(1+i\delta)/2} \exp[-X_{p,q}(\tau)|\alpha_0|^2], \quad (2.12)$$

$$X_{p,q}(\tau) = \frac{\Delta \cosh(v\bar{\kappa}\Delta/2) - (1-i\delta)\sinh(v\bar{\kappa}\Delta/2)}{\Omega \sinh(v\Delta\bar{\kappa}/2) + \Delta \cosh(v\bar{\kappa}\Delta/2)}, \quad (2.13)$$

$$Y_{p,q}(\tau) = \frac{\Delta \cosh(v\bar{\kappa}\Delta/2) + (1+i\delta)\sinh(v\bar{\kappa}\Delta/2)}{\Omega \sinh(v\Delta\bar{\kappa}/2) + \Delta \cosh(v\bar{\kappa}\Delta/2)}, \quad (2.14)$$

and

$$\delta = (p - q) / \bar{\kappa}, \quad (2.15)$$

$$\Omega = (1 + 2\bar{n} + i\delta), \quad (2.16)$$

$$\Delta = \Omega^2 - 4\bar{n}(1 + \bar{n})^{1/2}, \quad (2.17)$$

$$v = 2\mu\tau, \quad (2.18)$$

$$\bar{\kappa} = \kappa / 2\mu. \quad (2.19)$$

In Figs. 5(a) and 5(b) we plot the Q function in Eq. (2.11) versus real and imaginary parts of α . In Fig. 5(a), $\bar{n} = 0$ and the interference fringes are still visible. As \bar{n} increases these fringes are diminished. At $\bar{n} = 10.0$, the classical whorl structure is clearly evident. This figure [5(b)] also shows some overall contraction due to the dissipative nature of the dynamics.

The Q function directly gives antinormally ordered moments:

$$\langle a^n (a^\dagger)^m \rangle = \int d^2\alpha \frac{1}{\pi} \alpha^n (\alpha^*)^m a(\alpha). \quad (2.20)$$

Using Eq. (2.11) one finds

$$\begin{aligned} \langle a_n(\tau) \rangle = & \alpha_0^n [Y_{n,0}(\tau)]^{-(n+1)} R_{n,0}(\tau) \\ & \times \exp \left[-|\alpha_0|^2 \frac{H_n^2(\tau)}{Y_{n,0}(\tau)} \right], \end{aligned} \quad (2.21)$$

where

$$H_n(\tau) = \frac{2\Delta_n e^{-v\bar{\kappa}\Delta_n/2}}{(\Omega_n + \Delta_n) - (\Omega_n - \Delta_n) e^{-v\bar{\kappa}\Delta_n}} \quad (2.22)$$

and Ω_n and Δ_n are given by Eqs. (2.16) and (2.17) with δ replaced by $n/\bar{\kappa}$.

The average energy in the oscillator is given by

$$\langle a^\dagger a \rangle = |\alpha_0|^2 e^{-v\bar{\kappa}} + \bar{n}(1 - e^{-v\bar{\kappa}}), \quad (2.23)$$

indicating an exponential approach to an equilibrium value of $\langle a^\dagger a \rangle = \bar{n}$.

In Figs. 6(a) and 6(b) we plot two average trajectories over the time interval, $0 \leq v \leq 24\pi$ on the phase space [that is, we plot the imaginary part of $\langle a(\tau) \rangle$ against the real part of $\langle a(\tau) \rangle$], for two values of $|\alpha_0|^2$ with $\bar{\kappa}$ and \bar{n} fixed. For fixed $\bar{\kappa}$ and \bar{n} as $|\alpha_0|^2$ increases there is a suppression of the recurrence at $v = 4\pi$. The fact that the

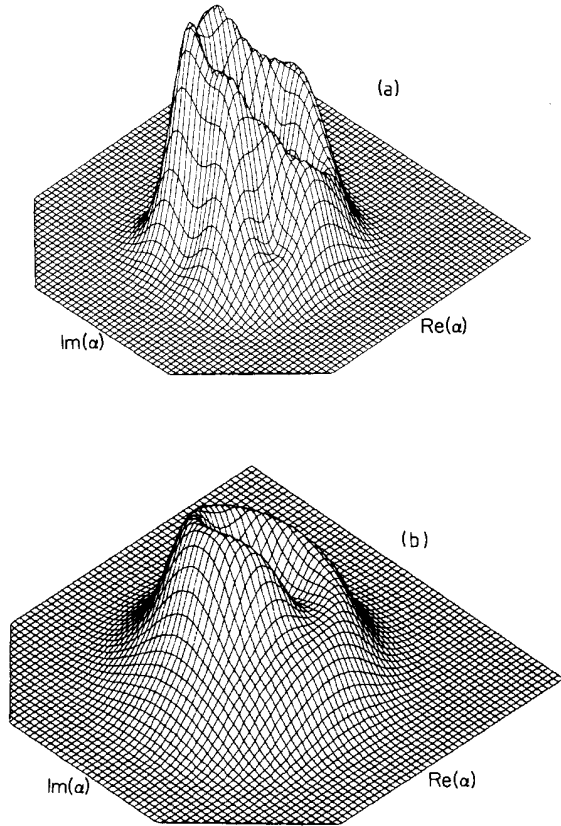


FIG. 5. Plot of the Q function vs real and imaginary parts of α for the dissipative nonlinear oscillator. (a) $\alpha_0=2.0$, $\bar{\kappa}=0.1$, $\bar{n}=0$; (b) $\alpha_0=2.0$, $\bar{\kappa}=0.1$, $\bar{n}=10.0$. In both cases $\nu=1.15$.

suppression of the recurrence becomes more efficient as the initial average energy of the oscillator increases is typical of the decay of a quantum-coherence feature and provides a “built-in” semiclassical limit.

In Figs. 7(a)–7(d) we plot the variance of x_1 as a function of ν for various values of $|\alpha_0|^2$, $\bar{\kappa}$, and \bar{n} . In all cases the variances decay to a value determined by the phase-independent fluctuations in the bath; thus the steady state variance is $V(x_i)_{ss}=0.5$. In Fig. 7(a) the decrease in fluctuations at ν , an odd multiple of π , together with a partial recurrence of the initial variance, persists for quite a few periods. However, for the larger value of $\alpha_0=2.0$ in Fig. 7(b), these quantum features are suppressed more quickly and appear only as diminishing dips on the exponential decay. The decay reflects the dissipative contraction of the density. This suppression is even more evident for larger values of α_0 [Figs. 7(c) and 7(d)]. We conclude that even for $\bar{n}=0$ the sharp reduction in fluctuations at $\nu=\pi$ will be considerably suppressed as $|\alpha_0|^2$ approaches the semiclassical scale.

The effect of attenuation on the quantum-coherence features discussed above is perhaps more clearly seen in the marginal distributions. In Sec. I we showed that for α_0 imaginary the marginal distribution for \hat{X}_1 contained

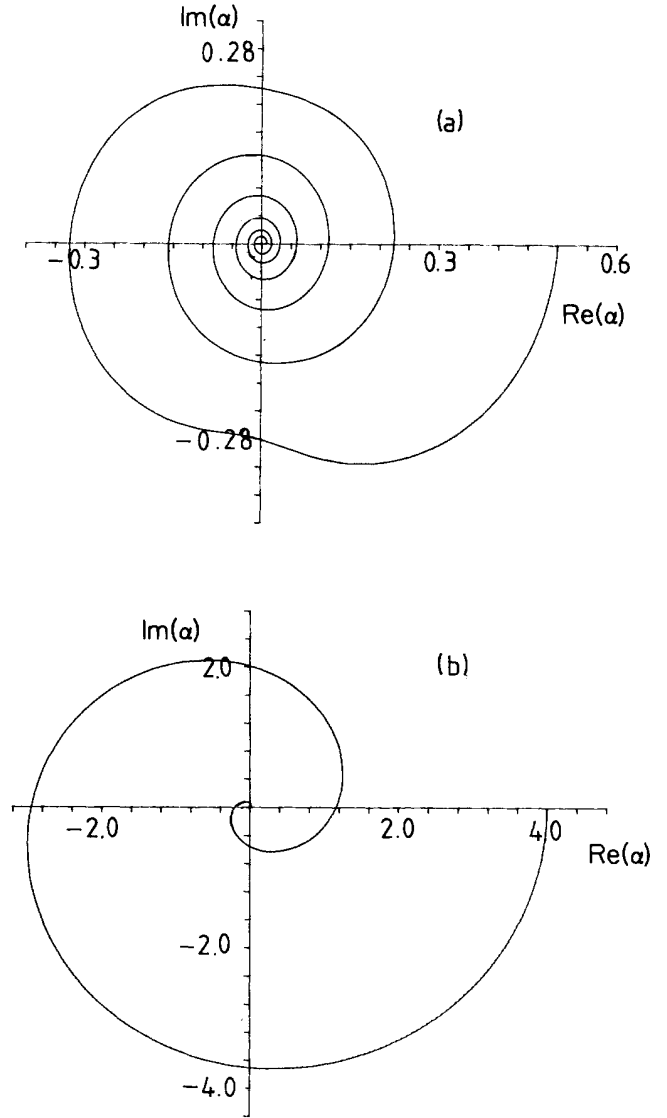


FIG. 6. Plot of imaginary $\langle \alpha(\tau) \rangle$ vs real $\langle \alpha(\tau) \rangle$ for the damped nonlinear oscillator. (a) $\alpha_0=0.5$, $\bar{\kappa}=0.1$, $\bar{n}=0$, $0 \leq \nu \leq 24\pi$; (b) $\alpha_0=4.0$, $\bar{\kappa}=0.1$, $\bar{n}=0.0$, $0 \leq \nu \leq 24\pi$.

interference features at $\nu=\pi$. We now calculate the marginal distributions in the presence of attenuation.

The matrix elements of the density operator in the basis $|X_1\rangle$ are given as phase-space integrals as

$$\langle X_1 | \hat{\rho} | X'_1 \rangle = \int d^2\alpha \frac{1}{\pi} \int d^2\beta \frac{1}{\pi} \langle X_1 | \alpha \rangle \langle \beta | X'_1 \rangle \langle \alpha | \hat{\rho} | \beta \rangle. \quad (2.24)$$

The off-diagonal coherent-state matrix elements are determined by the diagonal matrix elements $\langle \alpha | \hat{\rho} | \alpha \rangle$, the Q function, as follows. First, multiply the Q function by $e^{|\alpha|^2}$; secondly, replace α^* by β^* in the resulting expression; and finally, multiply this expression by

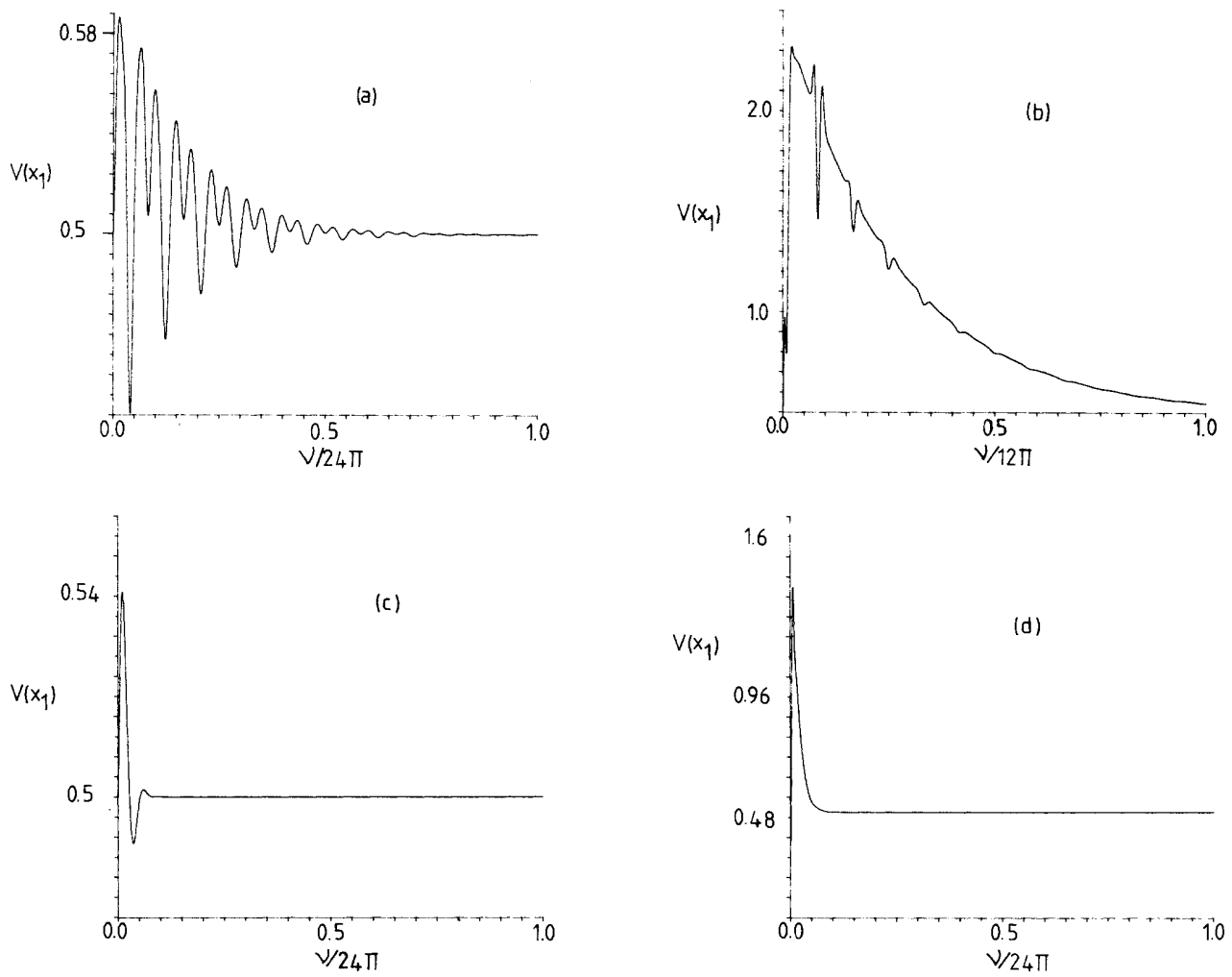


FIG. 7. Plot of the variance in x_1 , vs v . (a) $\alpha_0=0.5, \bar{\kappa}=0.1, \bar{n}=0.0$. (b) $\alpha_0=2.0, \bar{\kappa}=0.1, \bar{n}=0.0$. (c) $\alpha_0=0.5, \bar{\kappa}=1.0, \bar{n}=0.0$. (d) $\alpha_0=2.0, \bar{\kappa}=1.0, \bar{n}=0.0$.

$$\exp[-(|\alpha|^2 + |\beta|^2)/2].$$

The result in this case is

$$\langle \beta | \hat{\rho} | \alpha \rangle = \sum_{q,p=0}^{\infty} \frac{(\alpha \alpha_0^*)^q (\beta^* \alpha_0)^p}{q! p!} R_{p,q}(\tau) \times \exp\{\alpha \beta^* [1 - Y_{p,q}(\tau)] - \frac{1}{2}(|\alpha|^2 + |\beta|^2)\}, \quad (2.25)$$

where all the time-dependent functions are given in Eqs.

(2.12)–(2.19). The wave function $\langle X_1 | \alpha \rangle$ is given by¹⁷

$$\langle X_1 | \alpha \rangle = \left[\frac{2}{\pi} \right]^{1/4} \exp(-\frac{1}{2}|\alpha|^2 - X_1^2) \times \sum_{m=0}^{\infty} \frac{\alpha^m}{m!} 2^{-m/2} H_m(\sqrt{2}X_1), \quad (2.26)$$

where H_m is a Hermite polynomial of degree m . Substituting this result into Eq. (2.24) and evaluating the integrals we find

$$\langle X_1 | \hat{\rho}(\tau) | X_1' \rangle = \left[\frac{2}{\pi} \right]^{1/2} \sum_{q,p=0}^{\infty} \frac{(\alpha_0^*)^q (\alpha_0)^p}{q! p!} 2^{-(p+q)/2} R_{p,q}(\tau) e^{-(X_1^2 + X_1'^2)} \times \sum_{m=0}^{\infty} (2^m m!)^{-1} H_{m+p}(\sqrt{2}X_1) H_{m+q}(\sqrt{2}X_1') [Z_{p,q}(\tau)]^m, \quad (2.27)$$

where

$$Z_{p,q}(\tau) = \frac{2\bar{n}}{\Omega + \Delta \coth(v\bar{\kappa}\Delta/2)}. \quad (2.28)$$

This expression becomes the marginal probability density for X_1 , $P(X_1)$, when $X'_1 = X_1$.

As a useful check it is interesting to evaluate Eq. (2.27) when $\mu=0$, as this result has been previously obtained by Savage and Walls.²² To effect the comparison we note that when $\mu=0$ all the time-dependent functions, $f(t)$, $\eta(t)$, $X(\tau)$, and $Z(t)$ became independent of p and q .

The sum over the Hermite polynomials may then be performed using the summation formula

$$\sum_{q=0}^{\infty} \frac{U^q}{q!} \sum_{p=0}^{\infty} \frac{V^p}{p!} \sum_{m=0}^{\infty} (2^m m!)^{-1} H_{m+p}(\xi_1) H_{m+q}(\xi_2) z^m \\ = (1-z^2)^{-1/2} \exp(2\xi_1 V + 2\xi_2 U - V^2 - U^2) \exp \left[\frac{2z(\xi_1 - V)(\xi_2 - U) - z^2[(\xi_1 - V)^2 + (\xi_2 - U)^2]}{1-z^2} \right]. \quad (2.29)$$

Next we make the change of variable $X_1 = (\omega_0/2\hbar)^{1/2}(x-y)$ and $X'_1 = (\omega_0/2\hbar)^{1/2}(x+y)$. Then

$$\langle x-y | \hat{\rho}(\tau) | x+y \rangle = (2\pi\sigma_x^2)^{-1/2} \exp \left[\sigma_y^2 \delta_-^2 \frac{\omega}{\hbar} \right] \exp \left\{ -\frac{1}{2} \sigma_x^2 \left[x - \left[\frac{\hbar}{2\omega} \right]^{1/2} \delta_+ \right]^2 - \frac{1}{2} \sigma_y^2 \left[y - \sigma_y^2 \left[\frac{2\omega}{\hbar} \right]^{1/2} \delta_- \right]^2 \right\}, \quad (2.30)$$

where

$$\sigma_x^2 = \frac{\hbar}{2\omega} [2\bar{n} + (1 - e^{-v\bar{\kappa}}) + 1], \quad (2.31)$$

$$\sigma_y^2 = \frac{\hbar}{2\omega} [2\bar{n}(1 - e^{-v\bar{\kappa}}) + 1]^{-1}, \quad (2.32)$$

$$\delta_+ = (\alpha_0^* + \alpha_0) e^{-v\bar{\kappa}/2}, \quad (2.33)$$

$$\delta_- = (\alpha_0^* - \alpha_0) e^{-v\bar{\kappa}/2}. \quad (2.34)$$

Equation (2.30) agrees with the result obtained by Savage and Walls.²²

In Figs. 8(a) and 8(b) we plot the marginal distribution $P(X_1)$ for various values of $\bar{\kappa}$, \bar{n} , and $|\alpha_0|^2$. We see that for fixed $\bar{\kappa}$ and \bar{n} interference fringe visibility decreases with increasing $|\alpha_0|^2$ as one expects for such a quantum-coherence effect. These plots should be compared to the $\bar{\kappa}=0$ case shown in Fig. 4(b).

B. Amplifier

The solution to Eq. (2.9) subject to the initial condition (2.10) is (see the Appendix)

$$Q(\alpha, \alpha^*, \tau) = \exp(-|\alpha|^2 - |\alpha_0|^2) \sum_{q,p=0}^{\infty} \frac{(\alpha\alpha_0^*)^q (\alpha^*\alpha_0)^p}{q! p!} e^{|\alpha|^2 Z_{p,q}(\tau)} P_{p,q}(\tau), \quad (2.35)$$

where

$$P_{q,p}(\tau) = e^{v\bar{\kappa}[\Omega/2 - (\bar{n}+1)]} \left[\frac{2\Delta e^{-v\bar{\kappa}\Delta/2}}{(\Omega+\Delta) - (\Omega-\Delta)e^{-v\bar{\kappa}\Delta}} \right]^{(q+p+1)} \exp \left[\frac{2\bar{n}|\alpha_0|^2(1 - e^{v\Delta\bar{\kappa}})}{(\Omega-\Delta) - (\Omega+\Delta)e^{-v\bar{\kappa}\Delta}} \right]^{(q+p+1)}, \quad (2.36)$$

$$Z_{p,q}(\tau) = \frac{2(1+\bar{n})(1 - e^{v\Delta\bar{\kappa}})}{(\Omega-\Delta) - (\Omega+\Delta)e^{-v\bar{\kappa}\Delta}}, \quad (2.37)$$

and δ , Ω , and Δ are given in Eqs. (2.15)–(2.19). When $\bar{n}=0$ we have $\Omega = \Delta = 1 + i\delta$ and Eqs. (2.36) and (2.37) become

$$P_{q,p}(\tau) = e^{-v\bar{\kappa}} e^{-v\bar{\kappa}\Omega(p+q)/2}, \quad (2.38)$$

$$Z_{p,q}(\tau) = \frac{1 - e^{-v\bar{\kappa}\Omega}}{\Omega}. \quad (2.39)$$

The time-dependent moments corresponding to the solution in Eq. (2.35) are given by

$$\langle a^n(\tau) \rangle = \alpha_0^n P_{n,0}(\tau) [1 - Z_{n,0}(\tau)]^{-(n+1)} \\ \times \exp \left[-|\alpha_0|^2 \frac{Z_{n,0}(\tau)}{Z_{n,0}(\tau) - 1} \right]. \quad (2.40)$$

The average energy is given by

$$\langle a^\dagger a \rangle = |\alpha_0|^2 e^{v\bar{\kappa}} + (e^{v\bar{\kappa}} - 1)(\bar{n} + 1), \quad (2.41)$$

indicating the expected exponential energy growth due to amplification.

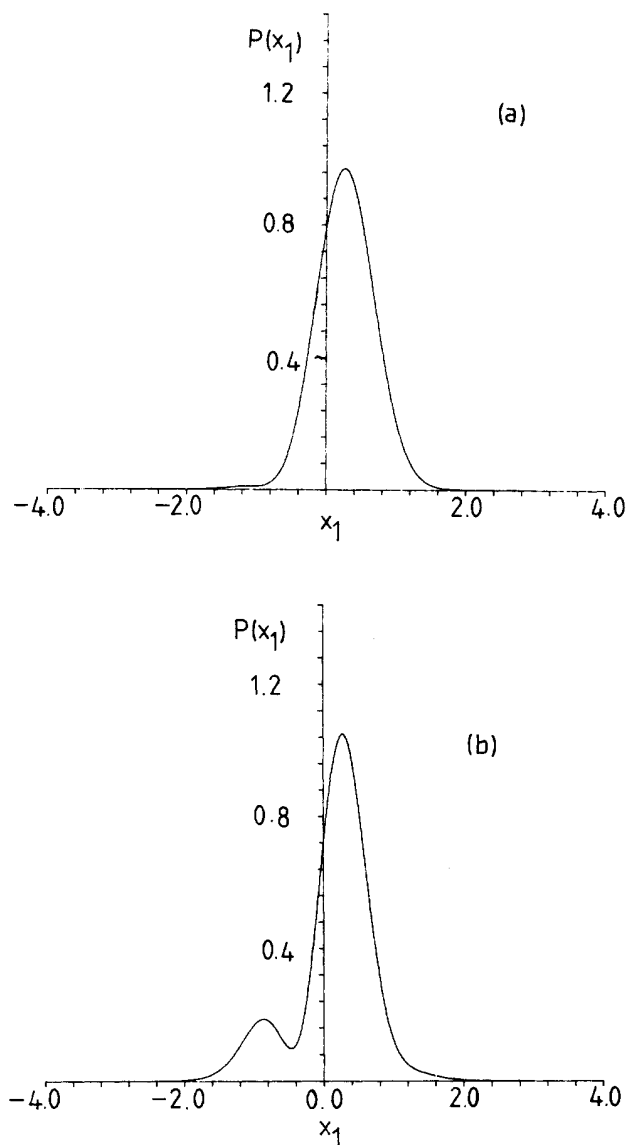


FIG. 8. Plot of the marginal distributions $P(x_1)$ for the attenuated nonlinear oscillator $\kappa=0.1$, $\nu=\pi$, $\bar{n}=0$. (a) $\alpha=0.5i$. (b) $\alpha=1.0i$.

In Figs. 9(a)–9(c) we plot the Q -function solution in Eq. (2.35) versus the real and imaginary parts of α , with $\alpha_0=2.0$ and various values of $\bar{\kappa}$ and \bar{n} . The restoration of the classical whorl structure becomes quite evident as $\bar{\kappa}$ increases even for this small value of α_0 . The density also reveals an overall dilation due to the amplification process, and also some broadening. In Fig. 9(c) the classical whorl structure is clearly evident with no hint of interference fringes.

In Fig. 10 we plot the mean trajectory $\langle a(\tau) \rangle$ on phase space over the time interval $0 \leq \nu \leq 24\pi$, for $\alpha_0=4.0$. Comparison of this figure with Fig. 6(b) seems to indicate

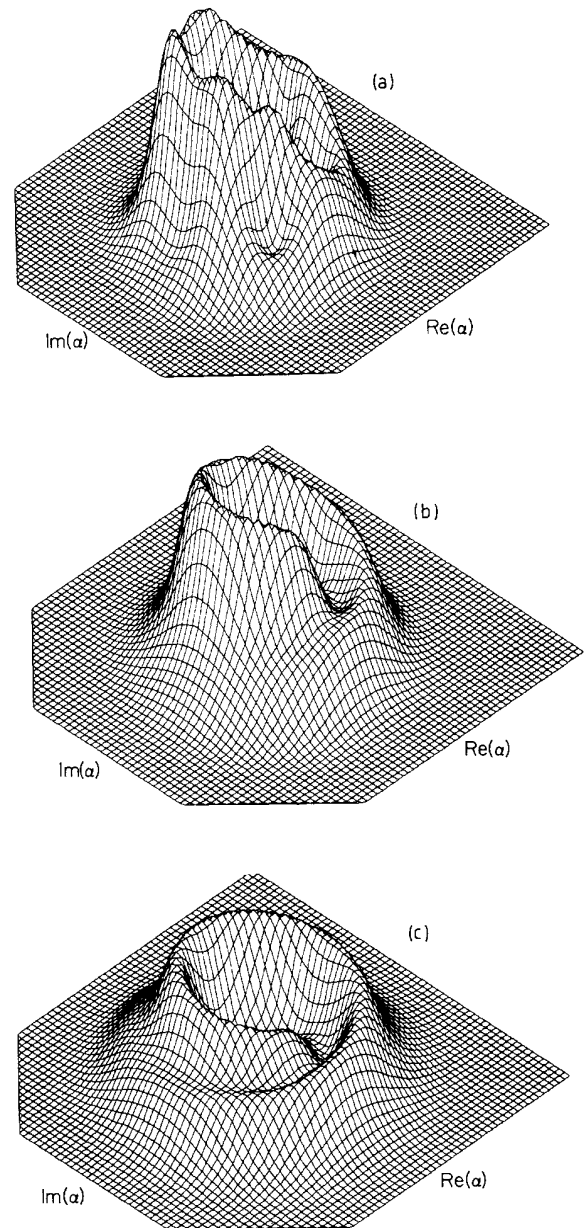


FIG. 9. Q -function solution for the amplifier at $\nu=1.15$, $\alpha_0=2.0$. (a) $\bar{\kappa}=0.1$, $\bar{n}=0.0$. (b) $\bar{\kappa}=0.1$, $\bar{n}=2.0$. (c) $\bar{\kappa}=1.0$, $\bar{n}=0.0$.

that the recurrences in the amplifier are suppressed at a greater rate than those of the attenuator model. A similar effect can be seen in the variance $V(x_1)$ for the amplifier plotted in Fig. 11 [compare with the attenuator in Fig. 7(b)]. The coherence effects, the “bumps” on the curve, are suppressed more rapidly than in the corresponding damped case.

The greater effectiveness of the amplifier in suppressing quantum-coherence effects can be explained as follows.

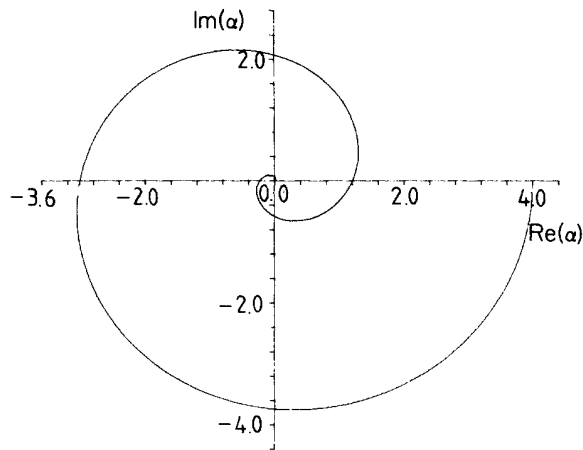


FIG. 10. Average trajectory for the amplified nonlinear oscillator. $\alpha_0=4.0, \bar{\kappa}=0.1, \bar{n}=0, 0 \leq \nu \leq 24\pi$.

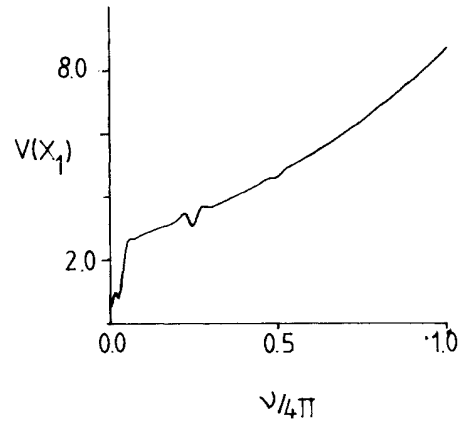


FIG. 11. Variance in x_1 vs $\nu/4\pi$ for the amplified nonlinear oscillator. $\alpha_0=2.0, \bar{\kappa}=0.1, \bar{n}=0.0$.

Firstly, to see more clearly the effect in the case of the mean trajectory it is instructive to consider the short-time approximation ($\nu\bar{\kappa} \ll 1$). In the case of the attenuator we find

$$\langle a(\tau) \rangle \simeq \alpha_0 e^{-i\nu/2} e^{-|\alpha_0|^2(1-e^{-i\nu})} e^{-|\alpha_0|^2\nu\bar{\kappa}e^{-i\nu}} \quad (\text{attenuator}),$$

while for the amplifier

$$\langle a(\tau) \rangle \simeq \alpha_0 e^{-i\nu/2} e^{-\nu\bar{\kappa}} e^{-|\alpha_0|^2(1-e^{-i\nu})} \times e^{-|\alpha_0|^2\nu\bar{\kappa}e^{-i\nu}} \quad (\text{amplifier}).$$

The amplifier moment contains an additional exponential

decay factor. The source of this extra decay factor is ultimately to be identified in the differing structures of the heat bath used in the two models. Coherence is diminished due to the random loss (in the attenuator model) or gain (in the amplifier model) of one quantum to or from the heat bath. In the case of the attenuator the rate of loss of quanta from the system depends on the number of quanta remaining in the system at any time; however, in the case of the amplifier even if there are no quanta in the system it can still gain a quantum of energy from the bath even for a zero-temperature bath. This may be seen more clearly by considering the contribution of the irreversible parts of the master equations [Eqs. (2.4) and (2.5)] to the rate of change of the matrix elements in the number state basis. For the case of the attenuator we find

$$\frac{\partial}{\partial \tau} \langle n | \hat{\rho}(\tau) | m \rangle = \dots + \frac{\bar{\kappa}}{2} [2\sqrt{(n+1)(m+1)} \langle n+1 | \hat{\rho} | m+1 \rangle - (n+m) \langle n | \hat{\rho} | m \rangle]$$

and for the amplifier we find

$$\frac{\partial}{\partial \tau} \langle n | \hat{\rho} | m \rangle = \dots + \frac{\bar{\kappa}}{2} [2\sqrt{(n-1)(m-1)} \langle n-1 | \hat{\rho} | m-1 \rangle - (n+m+2) \langle n | \hat{\rho} | m \rangle],$$

which shows an enhanced decay rate for the off-diagonal matrix element $\langle n | \hat{\rho} | m \rangle$. We conclude that a system subject to amplification will lose quantum coherence more rapidly than one subject to dissipation.

The marginal distributions for the amplifier model are determined by the solution in Eq. (2.35) in the same way as those for the attenuator model. The off-diagonal matrix elements in the basis which diagonalizes \hat{X}_1 are given by

$$\langle X_1 | \hat{\rho}(\tau) | X'_1 \rangle = \left[\frac{2}{\pi} \right]^{1/2} \exp\{-|\alpha_0|^2 - [X_1^2 + (X'_1)^2]\} \times \sum_{q,p=0}^{\infty} \frac{(\alpha_0^*)^q (\alpha_0)^p}{q! p!} P_{q,p}(\tau) 2^{-(p+q)/2} \sum_{m=0}^{\infty} (2^m m!)^{-1} H_{m+p}(\sqrt{2}X_1) H_{m+q}(\sqrt{2}X'_1) Z^m(\tau),$$

where $P_{q,p}(\tau)$ and $Z(\tau)$ are given in Eqs. (2.36) and (2.37).

In Figs. 12 we plot the marginal distribution $P(X_1) \equiv \langle X_1 | \hat{\rho} | X_1 \rangle$ at the time for maximum quantum

interference ($\tau = \pi/2\mu$) with $\alpha_0 = 2.0i$. Comparison of Figs. 8 and 12 shows that even for $\bar{n} = 0$ the visibility of the fringes decreases more significantly in the case of the amplifier nonlinear oscillator. This is consistent with the

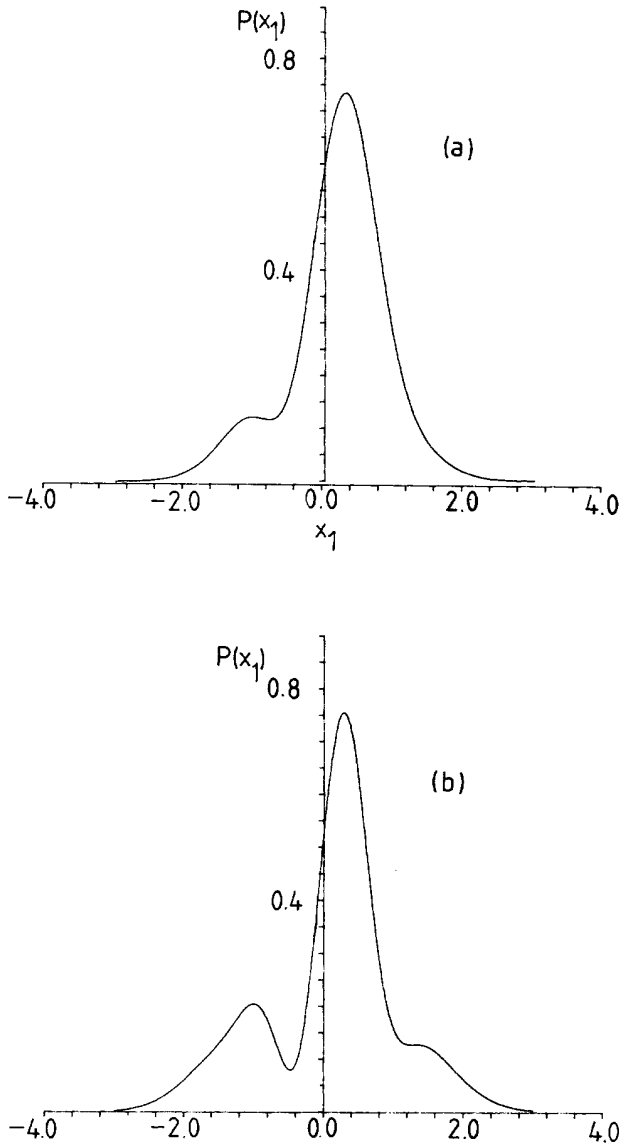


FIG. 12. Plot of the marginal distribution $P(X_1)$ for the amplified nonlinear oscillator. $\bar{\kappa}=0.1$, $\nu=\pi$, $\bar{n}=0.0$. (a) $\alpha_0=0.5i$. (b) $\alpha_0=1.0i$.

discussion above. Furthermore, we see that increasing $|\alpha_0|$ decreases fringe visibility as expected.

CONCLUSION

We have considered in this paper the effect of amplification and dissipation on a nonlinear oscillator model which exhibits a number of interesting quantum effects. These include recurrences of the initial state, squeezing, phase-space interference, and interference fringes in the marginal distributions of the canonical coordinates. We have considered the case of damping into a reservoir at nonzero temperature and also the case of amplification by a device at nonzero temperature. In both cases we confirm the previously established result that for given damping or amplification constants the rate of decay of coherence between superposed quantum states, as reflected in the quantum features listed above, becomes greater as the initial energy of the oscillator increases. This fact enables even small damping or amplification to restore classical behavior in the system as the semiclassical level is approached. We have also shown that amplification leads to a greater rate of coherence decay than does damping. As quantum-coherence features are most likely to occur in concert with very weak signals, amplification will form an essential part of any scheme to detect such effects. Our results show that only a limited amount of amplification can be tolerated before these quantum features are lost.

APPENDIX

This appendix contains the method of solution for the two Fokker-Planck equations [Eqs. (2.8) and (2.9)] corresponding to the attenuated nonlinear oscillator and the amplified nonlinear oscillator. We treat the attenuator case first.

The initial condition for solving Eqs. (2.8) is taken to be

$$Q(\alpha, \alpha^*, 0) = e^{-|\alpha - \alpha_0|^2}. \quad (\text{A1})$$

Let

$$Q(\alpha, \alpha^*, \tau) = p(\alpha, \alpha^*, \tau) e^{-|\alpha|^2 - |\alpha_0|^2}. \quad (\text{A2})$$

Then

$$\begin{aligned} \frac{\partial p}{\partial t} = i\mu \left[\alpha \frac{\partial p}{\partial \alpha} - \alpha^* \frac{\partial p}{\partial \alpha^*} + \alpha^2 \frac{\partial^2 p}{\partial \alpha^2} - (\alpha^*)^2 \frac{\partial^2 p}{\partial \alpha^{*2}} \right] + \frac{\kappa}{2} \left[- \left[\alpha \frac{\partial p}{\partial \alpha} + \alpha^* \frac{\partial p}{\partial \alpha^*} \right] + 2 \frac{\partial^2 p}{\partial \alpha \partial \alpha^*} \right] \\ + \kappa \bar{n} \left[-p + |\alpha|^2 - \left[\alpha^* \frac{\partial p}{\partial \alpha^*} + \alpha \frac{\partial p}{\partial \alpha} \right] + \frac{\partial^2 p}{\partial \alpha \partial \alpha^*} \right]. \end{aligned} \quad (\text{A3})$$

Now assume

$$p(\alpha, \alpha^*, \tau) = \sum_{q,p=0}^{\infty} \frac{(\alpha \alpha_0^*)^q (\alpha^* \alpha_0)^p}{q! p!} e^{|\alpha|^2 f(\tau)} p_{q,p}(\tau), \quad (\text{A4})$$

where $f(\tau)$ and $p_{q,p}(\tau)$ are functions of τ to be determined. The initial condition, Eq. (A1), requires that $f(0)=0$ and $p_{q,p}(0)=1$. Substituting Eq. (A4) into Eq. (A3) we may eliminate the α dependence to arrive at

$$\begin{aligned} \frac{\partial p_{q,p}}{\partial \tau} + qp \frac{\partial f(\tau)}{\partial t} p_{q,p} = & -i\mu \{ [q-p+q(q-1)-p(p-1)] p_{q,p} + 2qp(q-p)f(\tau) p_{q,p} \} \\ & + \frac{\kappa}{2} \{ -(q+p)p_{q,p} + 2|\alpha_0|^2 p_{q+1,p+1} + 2(q+p+1)f(\tau)p_{q,p} + 2qp[-2f(\tau)+f^2(\tau)] p_{q,p} \} \\ & + \bar{n} \{ -(q+p+1)p_{q,p} + |\alpha_0|^2 p_{q+1,p+1} + (q+p+1)f(\tau)p_{q,p} \\ & + qp[p_{q,p} - 2f(\tau)p_{q,p} + f^2(\tau)p_{q,p}] \} . \end{aligned} \quad (\text{A5})$$

Despite the formidable appearance of this equation the solution is obtained rather easily if we let

$$\frac{\partial f(\tau)}{\partial \tau} = \kappa(1+\bar{n})f^2(\tau) - \kappa[1+2\bar{n}+2i\mu(p-q)/\kappa]f(\tau) + \kappa\bar{n} . \quad (\text{A6})$$

Then

$$\begin{aligned} \frac{\partial p_{q,p}(\tau)}{\partial \tau} = & -\frac{\kappa}{2}(q+p)[1+2i\mu(p-q)/\kappa]p_{q,p}(\tau) + \kappa[(\bar{n}+1)f(\tau) - \gamma\bar{n}](q+p+1)p_{q,p}(\tau) \\ & + \kappa(1+\bar{n})|\alpha_0|^2 p_{q+1,p+1}(\tau) . \end{aligned} \quad (\text{A7})$$

To solve (A6) we let

$$\begin{aligned} \Omega &= 1+2\bar{n}+i\delta , \\ \Delta &= [\Omega^2 - 4\bar{n}(1+\bar{n})]^{1/2} , \end{aligned}$$

where

$$\delta = 2\mu(p-q)/\kappa .$$

Then using partial fractions the solution to Eq. (A6) is

$$f(\tau) = \frac{2\bar{n}}{\Omega + \Delta \coth(\kappa\Delta\tau/2)} . \quad (\text{A8})$$

To solve Eq. (A7) define $R_{q,p}(\tau)$ by

$$R_{q,p}(\tau) = G_{p,q}(\tau)p_{q,p}(\tau) , \quad (\text{A9})$$

where

$$G_{p,q}(\tau) = (e^{\kappa\bar{n}\tau - \kappa(1+\bar{n})F(\tau)})^{(q+p+1)} (\exp\{\kappa[1+2i\mu(p-q)\tau/\kappa]\})^{(p+q)/2} \quad (\text{A10})$$

and

$$F(\tau) \equiv \int_0^\tau f(\tau') d\tau' . \quad (\text{A11})$$

Then

$$\frac{dR_{q,p}(\tau)}{d\tau} = \{ (\kappa/2)(q+p)[1+2i\mu(p-q)/\kappa] + \kappa\bar{n}(q+p+1) - \kappa(\bar{n}+1)f(\tau) \} G_{p,q}(\tau)p_{p,q}(\tau) + G_{p,q}(\tau) \frac{\partial p_{p,q}(\tau)}{\partial t} . \quad (\text{A12})$$

Using the result for $\partial p_{q,p}/\partial \tau$ we obtain

$$\frac{\partial R_{q,p}(\tau)}{\partial \tau} = \kappa(1+\bar{n})|\alpha_0|^2 e^{-\kappa[1+2i\mu(p-q)/\kappa]\tau} e^{-2\kappa\bar{n}\tau} e^{2\kappa(\bar{n}+1)F(\tau)} p_{q+1,p+1}(\tau) . \quad (\text{A13})$$

Now take $R_{q,p} = R_{q+1,p+1}$ as this is compatible with the $t=0$ result and is a solution. Then

$$\frac{\partial R_{q,p}(\tau)}{\partial \tau} = \kappa(1+\bar{n})|\alpha_0|^2 e^{-\gamma\Omega\tau} e^{2\kappa(\bar{n}+1)F(\tau)} R_{q,p}(\tau) . \quad (\text{A14})$$

From Eq. (A8) we have

$$F(\tau) = \frac{-1}{\kappa(1+\bar{n})} \ln \left[\frac{(\Omega-\Delta) - (\Omega+\Delta)e^{\kappa\Delta\tau}}{(\Omega-\Delta) - (\Omega+\Delta)} \right] + \frac{2\bar{n}\kappa\Delta\tau}{\kappa\Delta(\Omega-\Delta)} . \quad (\text{A15})$$

From this we have

$$e^{2\kappa(1+\bar{n})F(\tau)} = \frac{4\Delta^2}{[(\Omega - \Delta) + (\Omega + \Delta)e^{\kappa\Delta\tau}]^2} e^{\kappa(\Omega + \Delta)\tau}, \quad (\text{A16})$$

which enables us to write Eq. (A14) as

$$\frac{dR_{q,p}(\tau)}{R_{q,p}} = \frac{-\kappa(1+\bar{n})}{(\Omega + \Delta)} \frac{1}{V^2} dV, \quad (\text{A17})$$

where

$$V = (\Omega - \Delta) + (\Omega + \Delta)e^{\kappa\Delta\tau} \quad (\text{A18})$$

and thus

$$R_{q,p}(\tau) = \exp \left[\frac{2(1+\bar{n})|\alpha_0|^2}{\Omega + \Delta \coth(\kappa\Delta\tau/2)} \right]. \quad (\text{A19})$$

Thus

$$p_{q,p}(\tau) = e^{-\kappa\bar{n}\tau} e^{\kappa\Omega\tau/2} \left[\frac{\Delta}{\Omega \sinh(\kappa\Delta\tau/2) + \Delta \cosh(\kappa\Delta\tau/2)} \right]^{(q+p+1)} \exp \left[\frac{2(1+\bar{n})|\alpha_0|^2}{\Omega + \Delta \coth(\kappa\Delta\tau/2)} \right]. \quad (\text{A20})$$

Putting this result into Eqs. (A4) and (A2) enables the solution quoted in Eq. (2.11) to be obtained.

The method of solution for the amplified case, Eq. (2.35), is very similar to that of the attenuator. We begin with the same initial condition and the same ansatz [Eqs. (A1) and (A2)]. We also assume a power-series expansion for $p(\alpha, \alpha^*, \tau)$ of the form given in Eq. (A4). The derivation is then quite similar to the attenuator case and for brevity we do not repeat it here.

¹G. J. Milburn, Phys. Rev. A **33**, 674 (1985).

²G. J. Milburn and C. A. Holmes, Phys. Rev. Lett. **56**, 2237 (1985).

³B. Yurke and D. Stoler, Phys. Rev. Lett. **57**, 13 (1986).

⁴A. O. Caldeira and A. J. Leggett, Phys. Rev. A **31**, 1059 (1985).

⁵W. H. Zurek, in *Proceedings of the International Symposium on the Foundations of Quantum Mechanics, Tokyo, 1982*, edited by S. Kamefuchi (Physical Society of Japan, Tokyo, 1983).

⁶D. F. Walls and G. J. Milburn, Phys. Rev. A **31**, 2403 (1985).

⁷C. M. Savage and D. F. Walls, Phys. Rev. A **32**, 2316 (1985).

⁸E. Joos and H. D. Zeh, Z. Phys. B **59**, 223 (1985).

⁹W. Schleich and J. A. Wheeler, Nature (London) **326**, 574 (1986); and see also W. Schleich and J. A. Wheeler, J. Opt. Soc. Am. B **4**, 1715 (1987).

¹⁰G. J. Milburn, in *Squeezed and Nonclassical Light*, edited by P. Tombesi and R. Pike (Plenum, New York, 1988).

¹¹K. Życkowski, Phys. Rev. A **35**, 3546 (1987).

¹²C. W. Gardiner, *Handbook of Stochastic Methods for Physics,*

Chemistry and the Natural Sciences (Springer, Berlin, 1985).

¹³M. Kitagawa, N. Imoto, and Y. Yamamoto, Phys. Rev. A **35**, 5270 (1987).

¹⁴E. B. Davies, *Quantum Theory of Open Systems* (Adademic, New York, 1986).

¹⁵G. J. Milburn, Phys. Rev. A **39** 2749 (1989).

¹⁶D. F. Walls, Nature (London) **306**, 141 (1983).

¹⁷W. H. Louisell, *Quantum Statistical Properties of Radiation* (Wiley, New York, 1973).

¹⁸R. P. Feynman and A. R. Hibbs, *Quantum Mechanics and Path Integrals* (McGraw-Hill, New York, 1965).

¹⁹R. J. Glauber, in *Laser Spectroscopy VIII*, edited by W. Persson and S. Svanberg (Springer, Berlin, 1987).

²⁰F. Haake, H. Risken, C. M. Savage, and D. F. Walls, Phys. Rev. A **34**, 3969 (1986).

²¹G. J. Milburn and D. F. Walls, Am. J. Phys. **51**, 1134 (1983).

²²C. M. Savage and D. F. Walls, Phys. Rev. A **32**, 2316 (1985).